© 2018. Published by The Company of Biologists Ltd | Journal of Cell Science (2018) 131, jcs222356. doi:10.1242/jcs.222356

RESEARCH ARTICLE

CAP1-mediated actin cycling via ADF/cofilin proteins is essential for asymmetric division in mouse oocytes

Zhe-Long Jin, Yu-Jin Jo, Suk Namgoong* and Nam-Hyung Kim*

ABSTRACT

Dynamic reorganization of the actin cytoskeleton is fundamental to a number of cellular events, and various actin-regulatory proteins modulate actin polymerization and depolymerization. Adenylyl cyclase-associated proteins (CAPs), highly conserved actin monomer-binding proteins, have been known to promote actin disassembly by enhancing the actin-severing activity of the ADF/cofilin protein family. In this study, we found that CAP1 regulated actin remodeling during mouse oocyte maturation. Efficient actin disassembly during oocyte maturation is essential for asymmetric division and cytokinesis. CAP1 knockdown impaired meiotic spindle migration and asymmetric division, and resulted in an accumulation of excessive actin filaments near the spindles. In contrast, CAP1 overexpression reduced actin mesh levels. CAP1 knockdown also rescued a decrease in cofilin family protein overexpression-mediated actin levels, and simultaneous expression of human CAP1 (hCAP1) and cofilin synergistically decreased cytoplasmic actin levels. Overexpression of hCAP1 decreased the amount of phosphorylated cofilin, indicating that CAP1 facilitated actin depolymerization via interaction with ADF/cofilin during mouse oocyte maturation. Taken together, our results provide evidence for the importance of dynamic actin recycling by CAP1 and cofilin in the asymmetric division of mouse female gametes.

This article has an associated First Person interview with the first author of the paper.

KEY WORDS: Actin, CAP1, ADF/cofilin, Oocyte, Asymmetric division

INTRODUCTION

The actin cytoskeleton consists of highly dynamic filament arrays, whose assembly and rapid turnover are essential during various stages of mammalian oocyte maturation, including asymmetric spindle migration, cortical actin cap formation, polar body extrusion and cytokinesis (Almonacid et al., 2014; Sun and Schatten, 2006; Yi and Li, 2012). Various actin-binding proteins play essential roles in the regulation of dynamic actin filament formation, elongation and depolymerization (Pollard and Borisy, 2003; Pollard and Cooper, 2009). For example, actin nucleators such as formin-2 (FMN2) (Dumont et al., 2007), SPIRE (Pfender et al., 2011) and the ARP2/3 complex (also known as ARPC) (Chaigne et al., 2015, 2013; Sun et al., 2011b) represent a family of proteins that initiate new actin filament formation and contribute to off-center meiotic spindle positioning. Whereas FMN2 and SPIRE are mainly involved in the formation of the cytoplasmic actin mesh network, the ARP2/3 complex (Chaigne et al., 2015, 2013; Sun et al., 2011b), JMY (Sun et al., 2011a) and N-WASP (Yi et al., 2011) are responsible for the cortical actin cap and subcortical actin network formation. In addition to actin nucleators, other actin-binding proteins, including capping proteins (Jo et al., 2015), tropomodulin (Jo et al., 2016), tropomyosins (Jang et al., 2014), and the actin depolymerizing factor (ADF)/cofilin protein family, have emerged as important factors in cytoplasmic actin mesh network maintenance in mouse oocytes.

Modulation of the dynamic balance between filamentous actin (F-actin) and globular actin (G-actin) is a central mechanism of actin cytoskeleton regulation. To recycle actin monomers, the F-actin filament is depolymerized to form G-actin. Filament severing is mediated by ADF/cofilin family proteins, which bind to the sides of filaments (Bernstein and Bamburg, 2010). In addition to ADF/cofilin proteins, several other proteins are involved in efficient actin filament recycling. One type of protein involved in the actin-severing pathway is the adenylyl cyclase-associated protein (CAP, also known as SRV2 in yeast) (Freeman and Field, 2000). CAP was first identified as a component of the yeast adenylyl cyclase complex that regulates both the actin cytoskeleton and the Ras/cAMP pathway (Fedor-Chaiken et al., 1990; Field et al., 1990). A recent study showed that CAPs enhanced actin monomer recharging with ATP antagonistically to ADF/cofilin (Ono, 2013), and they also promoted the severing of actin filaments in cooperation with ADF/cofilin (Chaudhry et al., 2013). Yeast and mammalian CAP homologues enhanced actin filament severing by 4–8-fold (Chaudhry et al., 2013; Jansen et al., 2014)

Two distinct mammalian CAP isoforms are known, CAP1 and CAP2 (Hubberstey and Mottillo, 2002; Yu et al., 1994, 1999). In mammals, CAP1 is expressed ubiquitously, excluding in the skeletal muscle, and CAP2 is predominantly expressed in the brain, heart, skeletal muscle and testes (Yu et al., 1994). Human CAP1 has been found to play a key role in accelerating actin filament turnover by effectively recycling cofilin family proteins (cofilin hereafter) and actin and by interacting with both ends of the actin filament (Moriyama and Yahara, 2002). CAP1 depletion leads to alterations in the actin cytoskeleton, cofilin and FAK phosphorylation, as well as increased cell adhesion and motility, and abnormal morphology in various cells (Bertling et al., 2004; Zhang et al., 2013). Mouse CAP1 forms hexameric structures that autonomously bind to F-actin, enhance cofilin-mediated severing, and catalyze the nucleotide exchange of actin (Jansen et al., 2014).

Considering the importance of CAPs in the actin dynamics of several cells, we investigated the role of CAP1 in the actin dynamics of murine oocyte maturation, where dynamic actin organization is crucial for spindle migration and asymmetric divisions.

Department of Animal Sciences, Chungbuk National University, Cheongju 361-763, Korea.

*Authors for correspondence (nhkim@chungbuk.ac.kr; suknamgoong@chungbuk.ac.kr)

Z.-L.J., 0000-0002-3408-0649; Y.-J.J., 0000-0002-9067-3537; S.N., 0000-0002-4395-5558; N.-H.K., 0000-0003-1741-9118

Received 5 July 2018; Accepted 23 October 2018

Journal of Cell Science (2018) 131, jcs222356. doi:10.1242/jcs.222356

RESULTS

CAP1 localized in the cytoplasm and at the cortical actin cap during mouse oocyte maturation

To investigate the functional role of CAP1 in mouse oocyte maturation, we first examined CAP1 subcellular localization during maturation. Oocytes were sampled at each developmental stage, corresponding to the mature germinal vesicle stage (GV), germinal vesicle breakdown (GVBD), metaphase I (MI) and metaphase II (MII). Subcellular localization of endogenous CAP1 was monitored via immunofluorescence staining. CAP1 showed punctate distribution throughout the entire cytoplasm during all oocyte developmental stages (Fig. 1A). CAP1 was also enriched at the cortical actin cap during the MI stage (Fig. 1B; Fig. S1). To confirm CAP1 localization, we expressed exogenous mScarlet-fused human CAP1 (mScarlet–hCAP1) in MI mouse oocytes. mScarlet–hCAP1 was dispersed throughout the cytoplasm and at the actin cap (Fig. 1C), supporting the immunostaining localization results.

Knockdown of CAP1 induced meiotic arrest and impaired asymmetric division of oocytes

Previously, CAP1 depletion in somatic cells has been shown to lead to F-actin accumulation and cytoskeletal defects (Zhang et al., 2013). Therefore, to investigate the function of CAP1 during mouse meiotic maturation, we depleted CAP1 mRNA by introducing CAP1 siRNA into oocytes. We confirmed via western blotting (1.21±0.1 vs 0.52±0.4; mean±s.e.m.), immunostaining, and qPCR analyses (1.04±0.04 vs 0.12±0.05) that siRNA introduction caused CAP1 mRNA and protein depletion (Fig. 2A–C). CAP1 knockdown (CAP1 KD) oocytes frequently exhibited multiple polar bodies, abnormally large polar bodies, or membrane bleb (Fig. 2D,E). Co-injection of mScarlet–hCAP1 was shown to rescue these defects (Fig. 2D–H), with abnormal polar body extrusion rates of: control, 6.06±3.03%; CAP1 KD, 31.72±3.51%; rescue: 13.92±3.08% (Fig. 2G). Subsequently, we examined the effect of CAP1 knockdown on mouse oocyte maturation. The maturation rate of oocytes injected with CAP1 siRNA was lower than that of control oocytes. The percentage of oocytes that matured to the MII stage was significantly decreased in the CAP1-knockdown oocytes (Fig. 2I,J), with polar body extrusion rates of: control, 87.62±4.72%; CAP1 KD, 58.87±8.1%; rescue, 81.89±1.1% (Fig. 2J). Moreover, the ratio of polar body diameter to oocyte diameter was significantly higher in the CAP1 knockdown oocytes, which was also rescued by mScarlet–hCAP1 injection (Fig. 2K). An abnormally large polar body was defined as having a diameter 50% greater than that of the oocyte. Collectively, these results indicated that CAP1 depletion negatively impacted mouse oocyte asymmetric division.

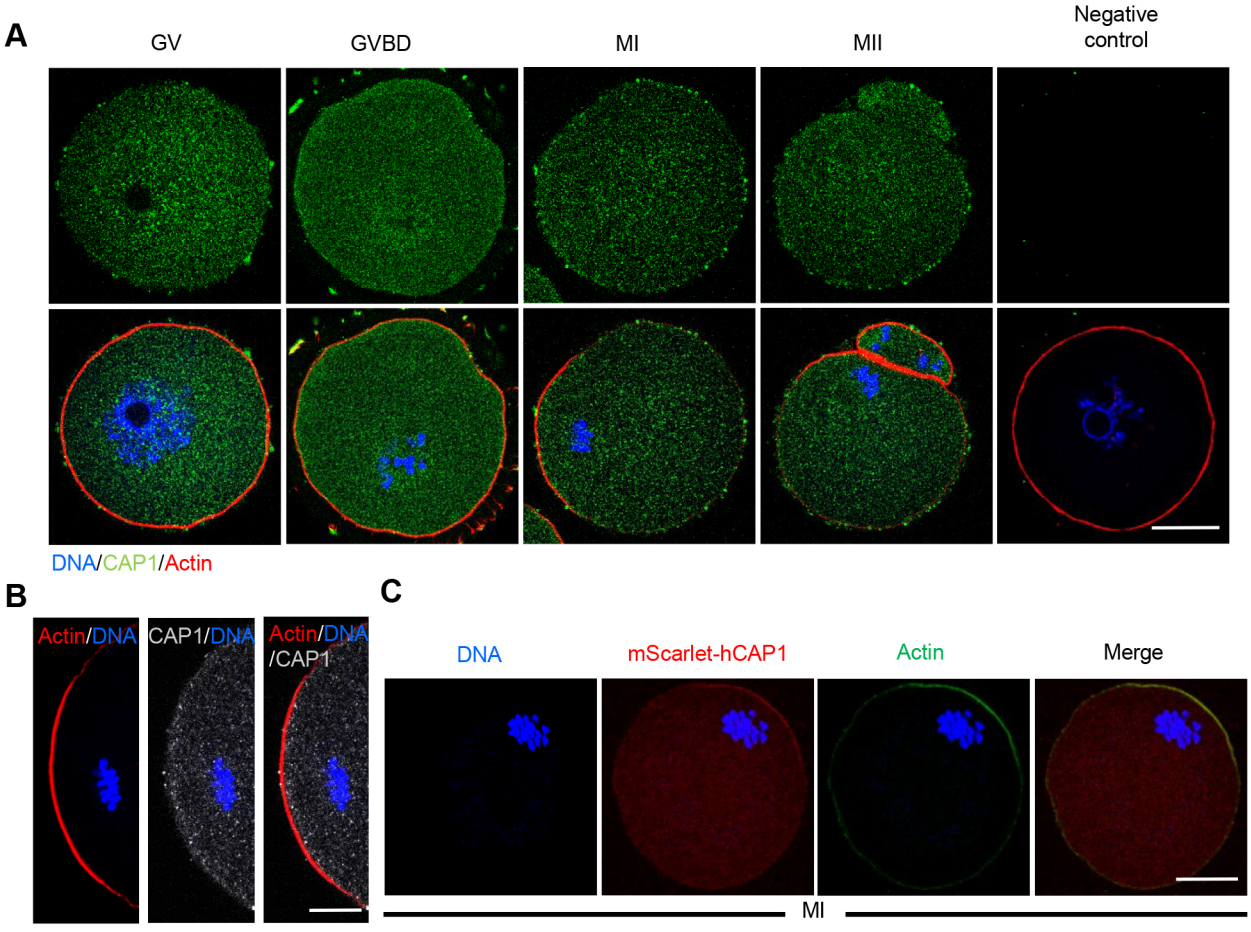

Fig. 1. CAP1 localization during mouse meiotic maturation. (A) Subcellular CAP1 localization during mouse oocyte meiosis, determined through staining with anti-CAP1 antibody. For the negative control, the anti-CAP1 primary antibody was omitted. CAP1 showed punctate distribution throughout the entire cytoplasm at all developmental stages. Blue, DNA; red, actin; green, CAP1. Scale bar: 20 µm. (B) Localization of CAP1 at the cortical actin cap in MI oocytes. Blue, DNA; red, actin; gray, CAP1. Scale bar: 10 µm. (C) Localization of mScarlet–human CAP1 (mScarlet–hCAP1) at MI oocytes. CAP1 was co-localized with actin in the cortical actin cap. Blue, DNA; green, actin; red, CAP1. Scale bar: 20 µm.

Journal of Cell Science (2018) 131, jcs222356. doi:10.1242/jcs.222356

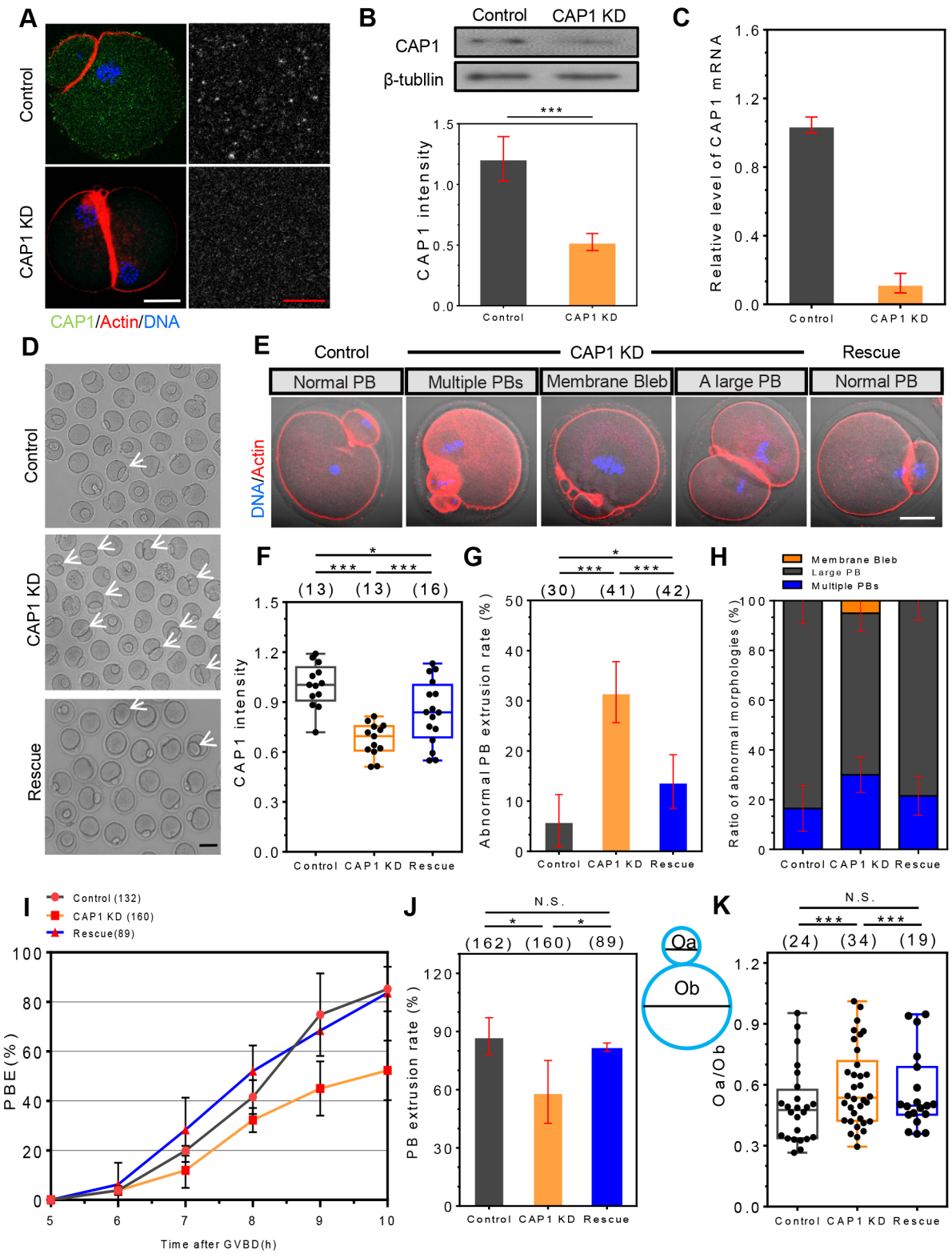

Fig. 2. See next page for legend.

Knockdown of CAP1 caused cytoplasmic actin mesh accumulation around the spindle during oocyte maturation and impaired spindle migration

Increased polar body size and symmetrical division is one of the main phenotypes associated with spindle migration failure in MI oocytes (Namgoong and Kim, 2016). Moreover, a dynamic cytoplasmic actin mesh is crucial for spindle migration during meiosis (Azoury et al., 2011, 2008). Therefore, we performed time-lapse microscopy to investigate the effects of CAP1 knockdown on spindle migration and dynamic cytoplasmic actin filament changes. The spindle moved from the center to near the cortex in control oocytes; however, in CAP1-knockdown oocytes, the spindle did not

Fig. 2. CAP1 is essential for asymmetric division during oocyte maturation. (A) Knockdown of CAP1 mRNA using siRNA injection. CAP1 immunostaining in negative control siRNA-injected (control) and CAP1 siRNA-injected MII oocytes shows CAP1 protein depletion in CAP1-knockdown oocytes. Green, CAP1; blue, DNA; red, actin. Scale bar: 20 µm. (B) Western blotting showed depletion of CAP1 protein levels in CAP1-knockdown oocytes compared with the control. Each lane contains protein extracted from 200 oocytes. Relative intensity of CAP1 was assessed using densitometry. Normalized expression of CAP1 is quantified from two independent experiments. ***P<0.001. (C) CAP1 mRNA levels in siRNA-injected oocytes (n=20) expressed relative to those in the negative control. Data in B,C indicate the mean±s.e.m. for three independent experiments. (D) The incidence of polar body extrusion (PBE) was quantified in the absence of milrinone after 13 h and is shown as representative images. Arrows indicate abnormal polar body extrusions. Scale bar: 50 µm. (E) Representative images of normal (control and rescue) and unusual (in response to CAP1 knockdown) oocyte morphologies at the MII stage are shown. Scale bar: 20 µm. (F–H) CAP1 western blot band intensity (F), rates of abnormal PBE (G), and ratio of abnormal morphologies (H) were quantified in control, CAP1-knockdown and CAP1-rescued oocytes. *P<0.05; ***P<0.001. (I,J) Timing (I) and rate (J) of PBE were determined in control, CAP1-knockdown and CAP1-rescued oocytes. *P<0.05; N.S., not significant. (K) The distribution of polar body diameter (Oa) to oocyte diameter (Ob) ratio in control, CAP1-knockdown and CAP1-rescued oocytes. ***P<0.001; N.S., not significant. The experiment was performed in triplicate and data in G–J are expressed as the mean±s.e.m. In F, K, box represents the 25–75th percentiles, and the median is indicated, whiskers show the range. The number of oocytes analyzed is specified in brackets.

move or moved extremely slowly, resulting in cytokinesis failure or 2-cell-like oocytes (Fig. 3A). Based on the average spindle movement in control (n=17) and CAP1-knockdown (n=22) oocytes (Fig. 3B,C), it is evident that spindle migration speeds increased between 8 h and 9 h in control oocytes. In contrast, CAP1-knockdown oocytes showed substantially delayed migration or were immobile. We confirmed the delay in spindle movements of CAP1-knockdown oocytes by measuring the distances between the spindle and cortex 9 h after the resumption of oocyte maturation and through spindle immunostaining (Fig. 3D,E). Further, to investigate the effect of CAP1 knockdown on cytoplasmic actin levels, control and CAP1-knockdown oocytes at the GVBD, MI and MII stages were sampled and stained with phalloidin. We found an abnormally high level of actin mesh accumulation around the spindle in CAP1-knockdown oocytes (Fig. 3F). The amount of cytoplasmic actin mesh in CAP1-knockdown oocytes was significantly increased during the GVBD, MI and MII stages (Fig. 3G). These CAP1-knockdown-mediated actin accumulations were rescued by co-injection with mScarlet–hCAP1 at the MI stage (Fig. 3H,I). These results indicate that the CAP1 knockdown impairs spindle migration and induces abnormal cytoplasmic actin mesh accumulation.

Disruption of cytokinesis by CAP1 knockdown during meiosis I

To gain more insight into how CAP1 knockdown disrupts cytokinesis, time-lapse imaging of maturing oocytes with the presence of an actin probe (GFP–UtrCH) was performed after GVBD. In control oocytes, chromosomes migrated close to the cortex and polar body extrusion (Fig. 4A; Movie 1). In CAP1-knockdown oocytes, chromosomes segregated and initiated cytokinesis, resulting in multiple polar bodies and two-cell-like oocytes (Fig. 4A; Movies 2, 3). Moreover, we found that in some oocytes, cytokinesis occurred and the cleavage furrow was not completely formed, resulting in the reincorporation of the protruding membrane into the oocyte, which resembled a single-cell-like morphology. Cytokinesis failure in CAP1-knockdown oocytes caused segregated chromosome assembly and abnormally high levels of surrounding cytoplasmic actin mesh (Fig. 4B,C). The rate of cytokinesis failure in CAP1-knockdown oocytes was significantly higher than in the control group (control, 0±0%; CAP1 KD, 17.67±1.45%) (Fig. 4D). Collectively, these data suggest that CAP1 knockdown negatively affects cytokinesis.

Overexpression of full length CAP1 decreased cytoplasmic actin mesh levels

To provide functional evidence for the role of CAP1 in actin remodeling during oocyte maturation, we overexpressed human CAP1 as a fusion protein with mNeongreen (mNeongreen–hCAP1) and evaluated its effect on oocyte maturation and cytoplasmic actin mesh density. The maturation rate of oocytes expressing mNeongreen–hCAP1 was not significantly different than that of control oocytes (Fig. 5A,B). However, CAP1 overexpression either increased the number of oocytes with multiple polar bodies or caused oocytes to undergo asymmetric division, similar to the phenotypes observed in the CAP1-knockdown oocytes, with abnormal polar body extrusion rates of: control, 4.97±1.63% (mean±s.e.m.); mNeongreen–hCAP1, 11.97±2.66% (Fig. 5C). Because CAP1 depletion can increase the cytoplasmic actin mesh density, even in an abnormal mesh, we examined whether CAP1 overexpression can reduce the amount of cytoplasmic actin mesh. MI oocytes were collected and stained with phalloidin (Fig. 5D). Oocytes overexpressing full-length CAP1 had significantly reduced cytoplasmic actin mesh levels (Fig. 5E). Moreover, cytokinesis failure was observed in CAP1-overexpressed oocytes (control, 0±0%; mNeongreen–hCAP1, 9.56 ±0.62%) (Fig. 5F,G). Using time-lapse imaging, we found in some oocytes overexpressing CAP1 that cytokinesis failed, but the chromosomes segregated and reassembled (Fig. 5H; Movies 4, 5), similar to phenotypes observed in some CAP1-knockdown oocytes shown in Fig. 4C. These results further support that proper CAP1 levels are essential to maintain the cytoplasmic actin mesh and to ensure cytokinesis during oocyte maturation.

Interaction of CAP1 with cofilin is required to maintain cytoplasmic actin mesh level

ADF/cofilin is a family of actin-binding proteins that cooperate with CAP1 and facilitate actin filament turnover (Moriyama and Yahara, 2002). Previously, non-phosphorylated cofilin levels were shown to be increased through inhibiting rho-associated kinase (ROCK), which impaired oocyte maturation (Duan et al., 2014), indicating a role of cofilin in oocyte maturation. However, the relationship between cofilin and its interaction partner CAP1 has not been investigated in mouse oocytes.

Because CAPs enhance the actin-severing activity of cofilin *in vitro* (Jansen et al., 2014), CAP1 knockdown in oocytes may complement excessive expression of active (S3A mutant) cofilin, which effectively decreases actin levels (Wang et al., 2017). We examined the amount of actin mesh under various conditions: CAP1 knockdown, constitutively active cofilin overexpression, and both CAP1 knockdown and cofilin overexpression. As expected, CAP1-knockdown oocytes showed increased actin accumulation, whereas cofilin-overexpressing oocytes showed decreased cytoplasmic actin levels. Upon simultaneous CAP1 knockdown and cofilin overexpression, actin levels increased as compared with cofilin-overexpressing oocytes, but not as much as in knockdown-only oocytes (Fig. 6A,B). These data indicate that the CAP1 knockdown-mediated increase in actin levels is related to cofilin activity.

We also tested the relationship between cofilin and CAP1 using the ROCK inhibitor Y-27632, which effectively increases non-phosphorylated cofilin levels (Duan et al., 2014). We observed a

Journal of Cell Science (2018) 131, jcs222356. doi:10.1242/jcs.222356

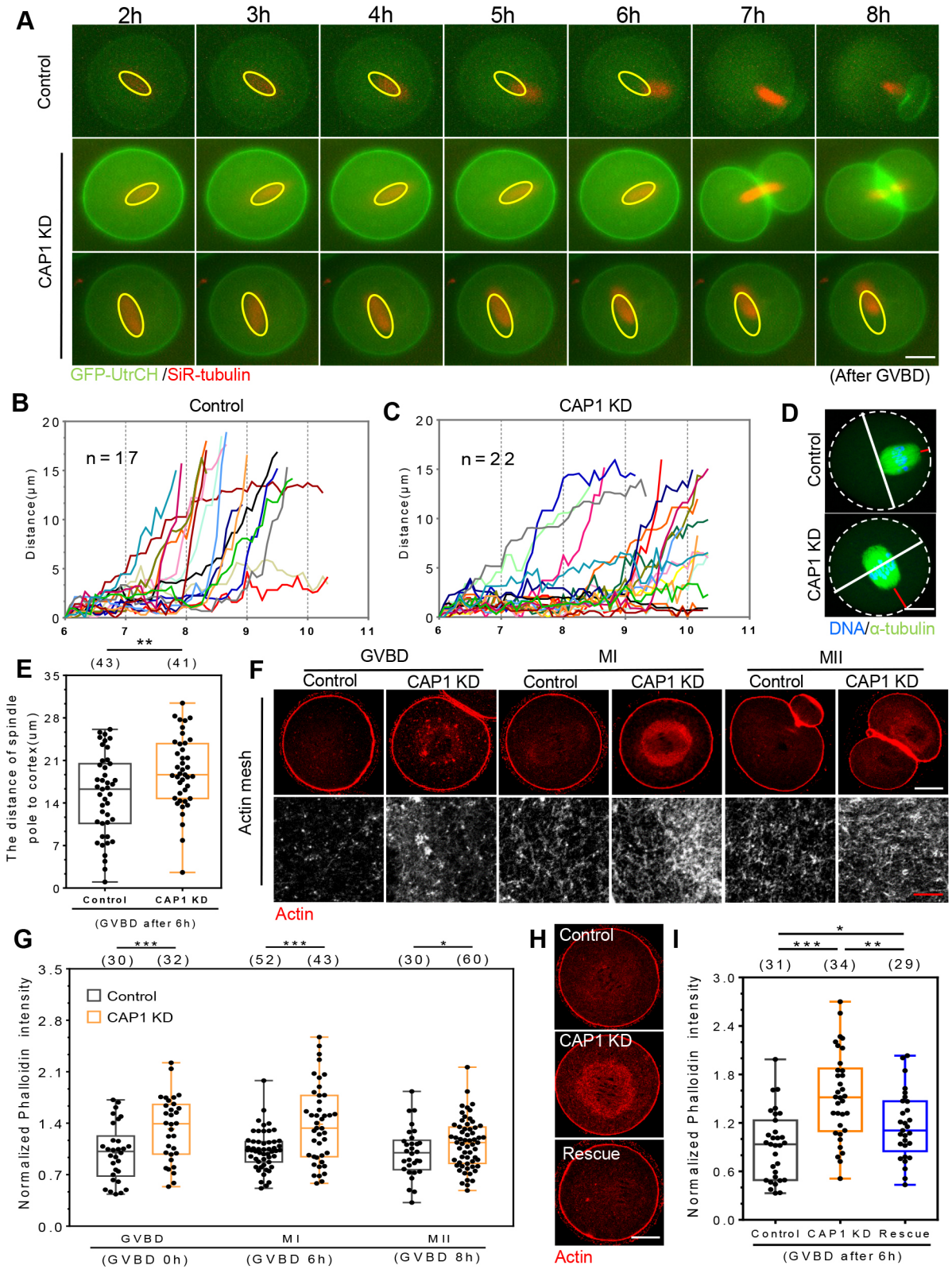

Fig. 3. See next page for legend.

similar significant decrease in the actin mesh level upon ROCK inhibitor (50 µM) treatment (Fig. 6C,D). However, simultaneous treatment of ROCK inhibitor and CAP1 knockdown did not show significant differences between only ROCK inhibitor-treated oocytes (Fig. 6C,D).

Further, we investigated the synergistic effects of mNeongreen–hCAP1 and cofilin–GFP (S3A) expression on cytoplasmic actin mesh disassembly in mouse oocytes and found that CAP1 enhanced cofilin-mediated disassembly. Simultaneous expression of mNeongreen–hCAP1 and cofilin–GFP (S3A) was found to elicit a greater decrease

Journal of Cell Science (2018) 131, jcs222356. doi:10.1242/jcs.222356

Fig. 3. CAP1 knockdown causes accumulation of cytoplasmic actin mesh around the spindle during oocyte maturation and impairs spindle migration. (A) Time-lapse microscopy of maturing control and CAP1-knockdown oocytes. GV oocytes were injection with GFP–UtrCH (actin, green) and stained with SiR-tubulin (red). Spindle locations after 2 h are marked with yellow ovals. Scale bar: 20 µm. (B,C) Tracking of spindle migration in control oocytes (B) and CAP1-knockdown oocytes (C). The distance (µm) of the spindle from its starting point at each time point is plotted. *n*-values are as indicated. (D) Control and CAP1-knockdown oocytes were sampled at 8.5 h after resumption of meiosis, and the location of spindles and DNA were confirmed using immunostaining of α-tubulin (green) and DNA (blue), respectively. The distance between the spindle pole and plasma membrane was marked with a red line. Dotted circle shows the oocyte boundary and white line indicates diameter of the oocyte parallel to the chromosome. Scale bar: 20 µm. (E) The distances between the spindle pole and plasma membrane were quantified in control and CAP1-knockdown oocytes. $^{**}P<0.01$. (F) The effects of CAP1-knockdown on the actin mesh level. Phalloidin staining of the cytoplasmic actin mesh at the 4 h (GVBD), 8 h (MI) and 12 h (MII). Magnified views of the cytoplasmic region are shown in the squares below. Scale bars: 20 µm (white), 3 µm (red). (G) Quantification of cytoplasmic actin via phalloidin fluorescence intensity at the GVBD, MI, and MII stages. $^{*}P<0.05$; $^{***}P<0.001$. (H) Phalloidin staining of the cytoplasmic actin mesh in control, CAP1-knockdown and CAP1-rescued MI oocytes. Scale bar: 20 µm. (I) Quantification of cytoplasmic actin via phalloidin fluorescence intensity in control, CAP1-knockdown and CAP1-rescued MI oocytes. $^{*}P<0.05$; $^{**}P<001$; $^{***}P<0.001$. The experiments were performed in triplicate, in graphs in E,G,I, the box represents the 25–75th percentiles, and the median is indicated, whiskers show the range. The number of oocytes analyzed is specified in brackets.

in the actin mesh level than separate expression (Fig. 6E,F), suggesting a synergy between CAP1 and cofilin in the maintenance of actin mesh levels. We further examined the potential effects on cofilin phosphorylation after CAP1 overexpression. Cofilin phosphorylation at Ser 3 was significantly decreased (Fig. 6G,H). Therefore, our results suggest that CAP1 is required to maintain the cytoplasmic actin mesh level through its interaction with cofilin.

DISCUSSION

CAPs are evolutionarily conserved actin cytoskeleton regulatory proteins with many suggested biochemical roles, including sequestering G-actin and enhancing nucleotide exchanges (Ono, 2013), enhancing actin filament severing (Chaudhry et al., 2013) and enhancing actin filament oligomerization (Balcer et al., 2003). The knockdown or knockout of CAPs have been shown to impair cell migration in mammalian cells (Bertling et al., 2004) or *Dictyostelium* (Noegel et al., 1999). It has also been reported that CAPs are involved in the actin cable assembly required for the endocytosis of yeast (Toshima et al., 2016). However, their functional role in mouse oocyte maturation, where actin remodeling-mediated spindle migration is crucial for asymmetric division, is unexplored. In this study, we provide evidence that CAP1 plays a crucial role in actin cytoskeleton remodeling during mouse oocyte maturation, presumably in collaboration with ADF/cofilin.

Depletion of CAP1 in mouse oocytes disrupted spindle migration, cortical actin cap formation and cytokinesis. Specifically, we observed the accumulation of excessive cytoplasmic actin mesh around spindles after CAP1 knockdown. The depletion of actin nucleators responsible for the formation of new actin filaments, such as FMN2 (Leader et al., 2002), SPIRE (Pfender et al., 2011) and the ARP2/3 complex (Sun et al., 2011b), or actin-binding proteins responsible for the maintenance of actin filaments, such as capping protein (Jo et al., 2015), tropomodulin (Jo et al., 2016), tropomyosin-3 (Jang et al., 2014) or filamin A (Wang et al., 2017) have been shown to impair asymmetric division by decreasing actin networks in oocytes. In contrast, excessive amounts of actin filaments in the cytoplasm have also been shown to be detrimental to spindle migrations, as seen with actin stabilization through GFP–UtrCH overexpression (Holubcová et al., 2013). The accumulation of actin filaments upon CAP1 knockdown corresponds to the role of CAP1 in facilitating the depolymerization of actin filaments.

Phosphorylated cofilin was distributed at the periphery of the spindle in mouse oocyte, which is consistent with previous work (Duan et al., 2018). We also found that CAP1 overexpression can decrease cofilin phosphorylation, which reduces actin mesh levels. Moreover, the expression of CAP1 and constitutively active cofilin synergistically decrease actin levels, indicating that the *in vivo* effect of CAP1 in mouse oocytes may be related to cofilin. The CAP1 knockdown phenotype is partially rescued by the overexpression of cofilin, suggesting that CAP1 may facilitate actin depolymerization by cofilin in mouse oocytes.

An intriguing observation from this study is that CAP1 localized in the cortex actin cap regions of mouse oocytes and was essential for actin cap formation and spindle migration. The cortical actin cap, which forms near the approaching spindle and promotes spindle positioning, contains a dense actin network (Yi et al., 2013; Yi et al., 2011). Cortical actin cap formation is dependent on the ARP2/3 complex, Rho family GTPases, and various nucleation-promoting factors (Leblanc et al., 2011; Wang et al., 2013). Previously, a CAP1-null mutation and mutations in the ARP2/3 complex pathway were shown to synergistically enhance morphological defects, suggesting that CAP1 is actively involved in ARP2/3-dependent actin regulation, or that CAP1 and ARP2/3 are involved in the same process (Deeks et al., 2007). CAP1 was also shown to be localized on the actin-rich lamellipodia of migration cells (Bertling et al., 2004; Freeman and Field, 2000), where ARP2/3-mediated actin polymerization and cofilin-mediated actin depolymerization is required (DesMarais et al., 2004). These results suggested that the dynamic nature of the actin cap structure is required for fast actin nucleation and depolymerization by ADF/cofilin, and that CAP1 may facilitate these processes during oocyte maturation.

It is clear that CAP1 is involved in actin filament depolymerization in mouse oocytes, but questions remained about how CAP1 is involved in this process. The most obvious interaction candidate is ADF/cofilin, which is the main driver of actin depolymerization in many cells. CAP1 has been shown to displace ADF/cofilin from ADP–actin monomers, which allowed for the recycling of ADF/cofilin for new rounds of filament depolymerization and actin monomers to replenish the assembly-competent pool of actin (Balcer et al., 2003). The N-terminal half of mouse CAP1 forms a hexameric structure with six symmetrical protrusions, and has been shown to sufficiently augment ADF/cofilin-mediated turnover and enhance cofilin-mediated severing by 8-fold (Jansen et al., 2014; Moriyama and Yahara, 2002). This activity was abolished with mutations at conserved surfaces on the HFD domain (Quintero-Monzon et al., 2009). Our data revealed similar results to previous studies. Co-expression of mNeongreen–hCAP1 and cofilin–GFP (S3A) elicited a greater decrease in the actin mesh level than separate expression (Fig. 6E). After CAP1 overexpression, cofilin phosphorylation decreased significantly (Fig. 6G,H), suggesting that CAP1 overexpression increases cofilin activity. Actin accumulation caused by CAP1 knockdown could also be rescued partially by cofilin overexpression, suggesting the possibility that some of the effect of CAP1 knockdown may be caused by cofilin. Previously, CAP1 and cofilin have not been successfully co-precipitated in IP assays (Zhang et al., 2013). Thus, further understanding of the molecular and biochemical mechanisms of the CAP1–cofilin interaction remained

Journal of Cell Science (2018) 131, jcs222356. doi:10.1242/jcs.222356

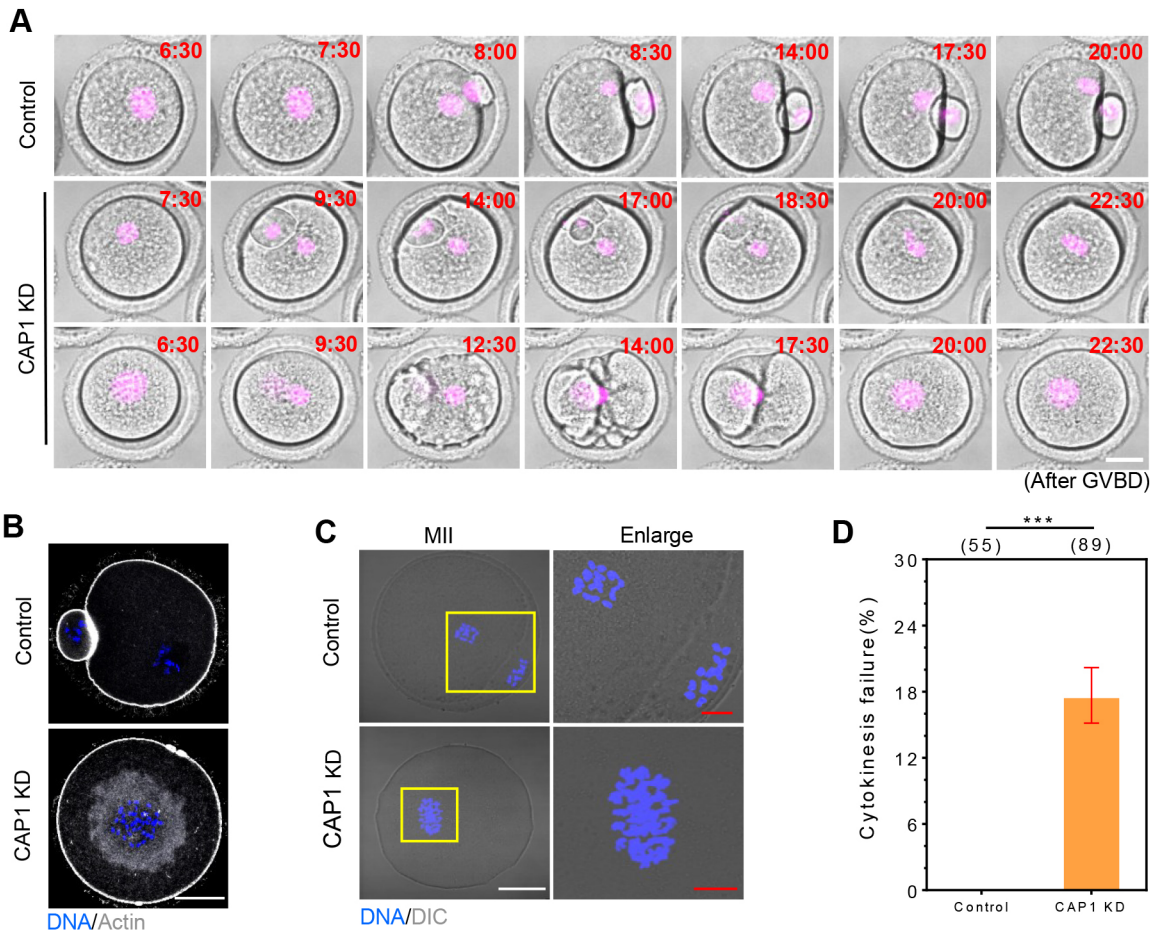

Fig. 4. CAP1 knockdown impairs cytokinesis during MI in mouse oocyte. (A) Chromatin tracking of maturing control and CAP1-knockdown oocytes via time-lapse microscopy. Chromatin was visualized through the injection of cRNA encoding H2B–mCherry (magenta). The upper panel corresponds to Movie 1, the middle panel corresponds to Movie 2 and the lower panel corresponds to Movie 3. Scale bar: 20 µm. (B) Control and CAP1-knockdown oocytes were sampled at 18 h, and the cytoplasmic actin mesh and DNA were visualized using immunostaining. Scale bar: 20 µm. (C) Control and CAP1-knockdown MII oocytes were sampled and the DNA was visualized using immunostaining. Magnified views of the oocyte DNA are shown in the squares to the right (yellow). Blue, DNA; DIC, differential interference contrast. Scale bar: 20 µm (white), 5 µm (red). (D) The rate of cytokinesis failure in oocytes after CAP1-knockdown is increased compared to that of control oocytes. ***P<0.001. The experiment was performed in triplicate and data are expressed as the mean±s.e.m. The number of oocytes analyzed is specified in brackets.

elusive. In addition, mouse N-CAP1 hexamers bind autonomously to F-actin, independent of cofilin. Under these conditions, N-CAP1 binding alters actin filament structure, leading to an increase in filament crossover distance and opposing the twisting effects of cofilin. These observations raise the possibility that N-CAP1 enhances severing by introducing local discontinuities in filament topology to accelerate cofilin-mediated fragmentation (Jansen et al., 2014). Moreover, another protein, twinfilin, has been found to catalyze depolymerization at the ends of actin filaments in concert with CAP (Johnston et al., 2015), indicating the possibility of a cofilin-independent mechanism of actin depolymerization by CAP. The presence and potential role of twinfilin in concert with CAP in mouse oocytes would need to be investigated further.

We also showed that hCAP1 overexpression reduced cofilin phosphorylation and decreased actin accumulation. It is not clear how hCAP1 overexpression reduced the phosphorylation levels of cofilin; however it has been suggested that the accumulation of cytoplasmic actin filaments may serve as a mechanism to protect cells by producing abnormally high cofilin activity (Zhang et al., 2013). CAP1 may be involved in cofilin activity regulation via interaction with slingshot phosphatase (Niwa et al., 2002), which dephosphorylates and activates cofilin.

Recently, actin filament reorganization has been implicated in proper chromosome segregation during meiosis I (Mogessie and Schuh, 2017). Considering that CAP1 knockdown resulted in the accumulation of actin filaments near the spindle and chromatin, CAP1-mediated actin depolymerization may be required for the proper segregation of chromosomes and prevention of segregation errors.

Collectively, our data showed that CAP1-mediated actin depolymerization activity is essential for spindle migration in mouse oocytes. This is the first report showing that ablation of actin depolymerization machinery impairs spindle migration in mouse oocytes by accumulation of actin filaments, demonstrating the importance of dynamic actin filament remodeling during oocyte maturation.

MATERIALS AND METHODS

Animals

All mice used in this study were 6–8-week-old ICR female mice. Animal care and handling were conducted in accordance with the policies regarding the care and use of animals issued by the ethics committee of the Department of Animal Science, Chungbuk National University, Korea.

Journal of Cell Science (2018) 131, jcs222356. doi:10.1242/jcs.222356

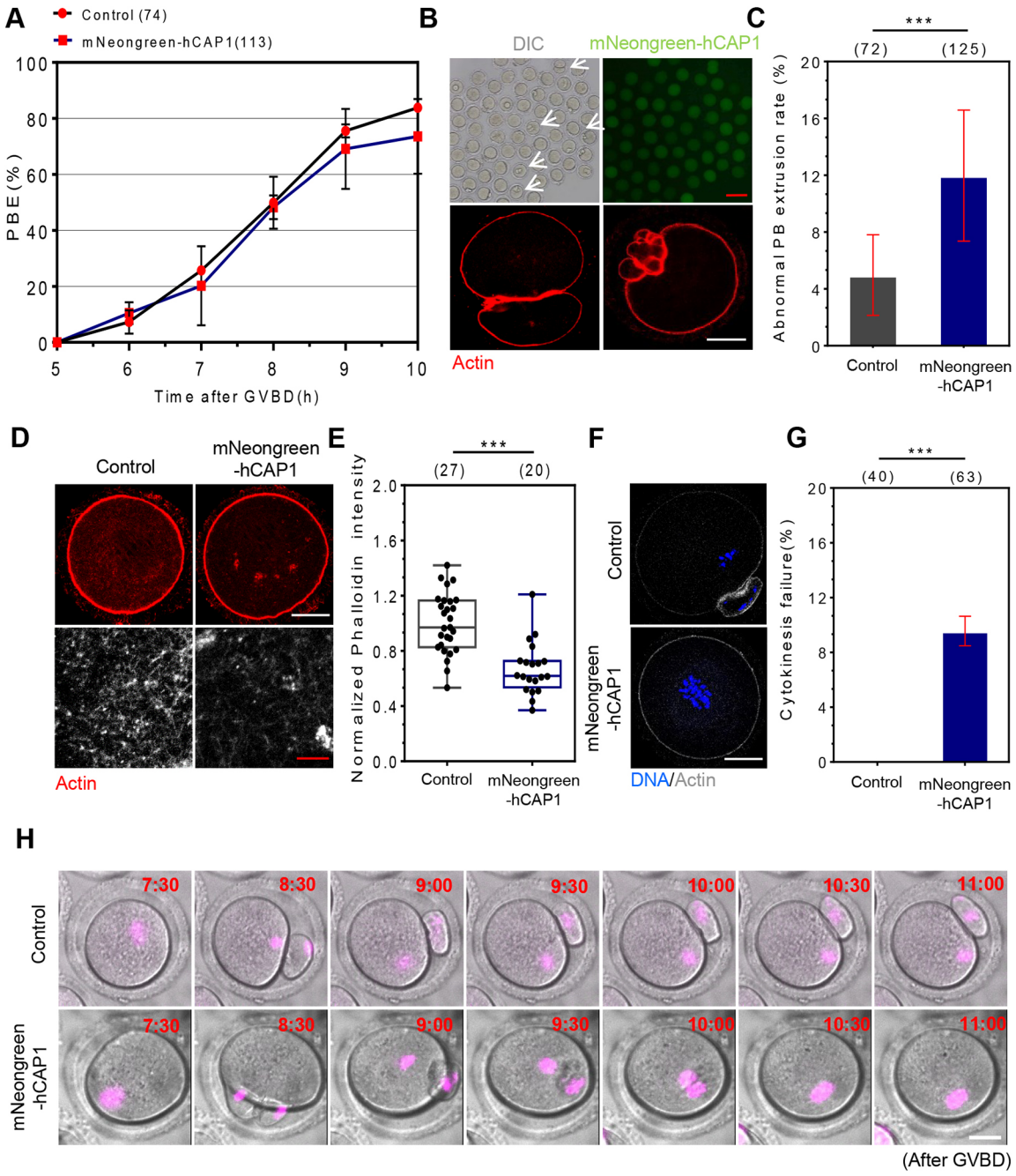

Fig. 5. Overexpression of full-length CAP1 affects the cytoplasmic actin mesh levels. (A) Timing of PBE was determined in control and CAP1-overexpressing (mNeongreen–hCAP1) oocytes. (B) mNeongreen–hCAP1 was injected into GV-stage oocytes and maturation was resumed. Representative DIC image of oocytes (top left) and mNeongreen–hCAP1 expression (top right). Arrows indicate abnormal MII oocytes. Phalloidin staining of cortical actin in mNeongreen–hCAP1-injected MII oocytes (bottom). Scale bars: 20 µm (white), 100 µm (red). (C) Rates of abnormal PBE were quantified in control and CAP1-overexpressing oocytes. ***P<0.001. (D) Phalloidin staining of the cytoplasmic actin mesh in control and CAP1-overexpressing MI oocytes. Magnified views of the cytoplasmic region are shown in the square below. Scale bars: 20 µm (white), 3 µm (red). (E) Quantification of cytoplasmic actin via phalloidin fluorescence intensity in control and CAP1-overexpressing oocytes. Box represents the 25–75th percentiles, and the median is indicated, whiskers show the range. ***P<0.001. (F) Control and CAP1-overexpressing oocytes were sampled at 13 h, and the cytoplasmic actin mesh and DNA were visualized using immunostaining. Scale bar: 20 µm. (G) The rate of cytokinesis failure in CAP1-overexpressing oocytes is increased compared to that of control oocytes. ***P<0.001. (H) Chromatin tracking of maturing control and CAP1-overexpressed oocytes via time-lapse microscopy. Chromatin was visualized through the injection of cRNA encoding H2B–mCherry (magenta). The upper panel corresponds to Movie 4 and the lower panel corresponds to Movie 5. Scale bar: 20 µm. The experiment was performed in triplicate and the data in C,G are expressed as the mean±s.e.m. The number of oocytes analyzed is specified in brackets.

Oocyte collection

Ovaries from 6–8-week-old female ICR mice were sliced open using a blade to release germinal vesicle (GV) oocytes, which were placed in M2 medium (Sigma-Aldrich, St Louis, MO, USA) supplemented with 2.5 µM milrinone to prevent germinal vesicle breakdown (GVBD) during microinjection. Only intact GV oocytes were collected for further studies. The selected oocytes were placed in M16 medium under liquid paraffin oil at 37°C in an atmosphere containing 5% CO_2 for specific incubation periods. All reagents and media were purchased from Sigma-Aldrich unless otherwise stated.

Journal of Cell Science (2018) 131, jcs222356. doi:10.1242/jcs.222356

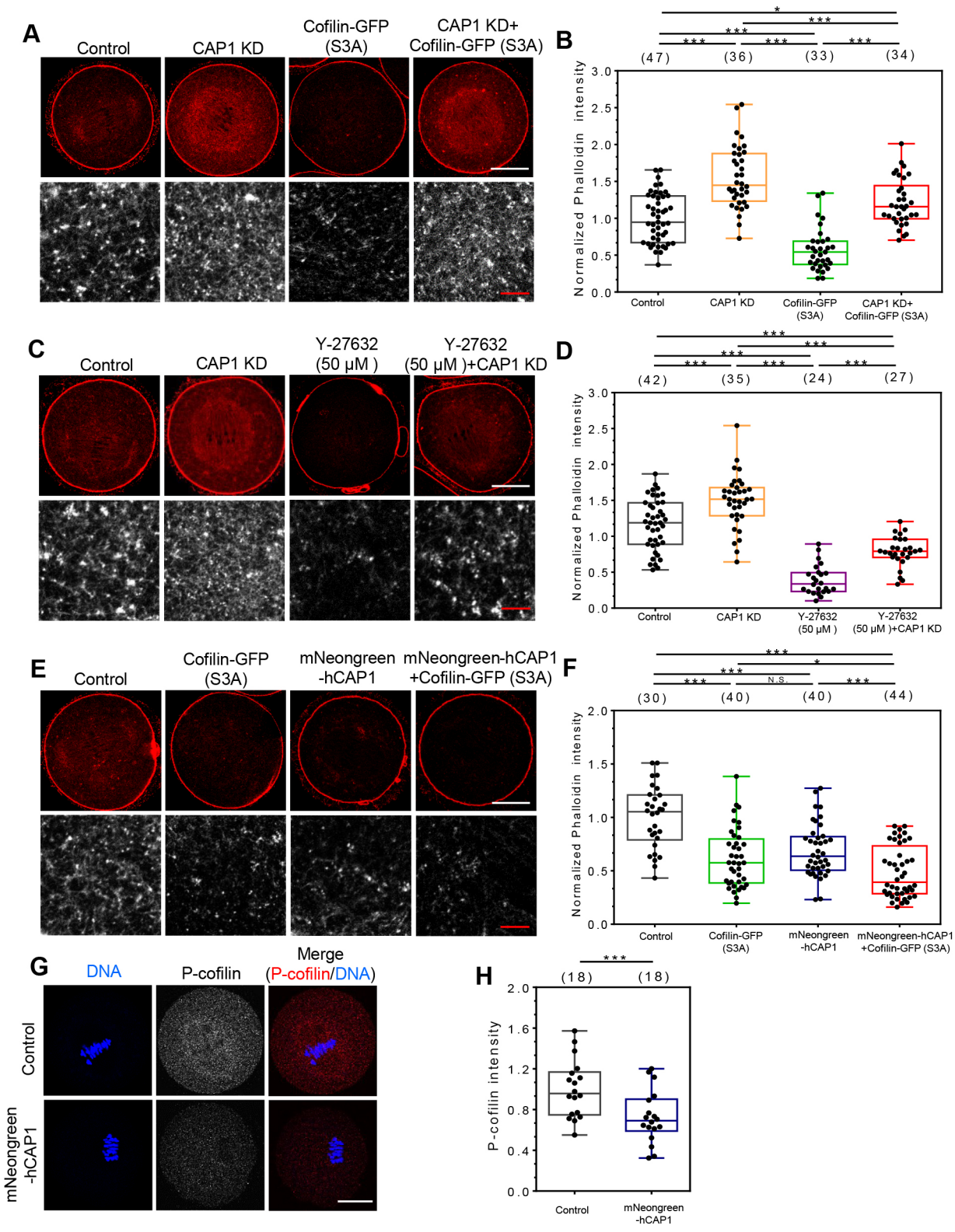

Fig. 6. See next page for legend.

Quantitative RT-PCR

Total RNA was extracted from 20 oocytes at each stage using the Dynabead mRNA DIRECT kit (Invitrogen, Grand Island, NY, USA). Corresponding cDNA was obtained via reverse transcription of the mRNA with a cDNA synthesis kit (Takara, Kyoto, Japan), using Oligo(dT)$_{12–18}$ primers and SuperScript III Reverse Transcriptase (Invitrogen). The primers used for real-time PCR (RT-PCR) were 5′-AAA CCT GGC CCC TTT GTG AA-3′ (forward) and 5′-TGA CCC AGT CCA CAT GCT TC-3′ (reverse). The amplification program was 95°C for 3 min followed by 35 cycles at 95°C for 15 s, 60°C for 30 s, and 72°C for 20 s, and a final extension step at 72°C for 5 min.

Fig. 6. Functional interactions between CAP1 and cofilin. (A) Phalloidin staining of the cytoplasmic actin mesh in MI oocytes injected with control siRNA (control), CAP1 siRNA (CAP1 KD), cofilin–GFP (S3A) and CAP1 siRNA+cofilin–GFP (S3A). Magnified views of the cytoplasmic region are shown in the squares below. Scale bars: 20 µm (white), 3 µm (red). (B) Quantification of cytoplasmic actin via phalloidin fluorescence intensity in oocytes injected with siRNA or cRNA. **P*<0.05; ****P*<0.001. (C) Phalloidin staining of the cytoplasmic actin mesh in MI oocytes treated with control siRNA (control), CAP1 siRNA or ROCK inhibitor Y-27632 (50 µM). Magnified views of the cytoplasmic region are shown in the squares below. Scale bars: 20 µm (white), 3 µm (red). (D) Quantification of cytoplasmic actin via phalloidin fluorescence intensity in MI oocytes. ****P*<0.001. (E) Phalloidin staining of the cytoplasmic actin mesh in MI oocytes injected with control siRNA (control), cofilin–GFP (S3A), mNeongreen–hCAP1 and cofilin–GFP (S3A)+mNeongreen–hCAP1. Magnified views of the cytoplasmic region are shown in the squares below. Scale bars: 20 µm (white), 3 µm (red). (F) Quantification of cytoplasmic actin via phalloidin fluorescence intensity in MI oocytes. **P*<0.05; ****P*<0.001; N.S., not significant (*P*>0.05). (G) Cofilin phosphorylation levels in control and CAP1-overexpressing (mNeongreen–hCAP1) oocytes after 8 h. Scale bar: 20 µm. (H) Quantification of phosphorylated (p)-cofilin fluorescence intensity in control and CAP1-overexpressing oocytes after 8 h. ****P*<0.001. The experiment was performed in triplicate, in graphs in B,D,F,H, the box represents the 25–75th percentiles, and the median is indicated, whiskers show the range. The number of oocytes analyzed is specified in brackets.

Drug treatment

A 5 mM solution of Y-27632 (Sigma-Aldrich) in water was diluted in M16 medium to a concentration of 50 mM. Oocytes were then cultured in this medium for various times. Control oocytes were cultured in fresh M16 medium.

siRNA injection

Approximately 5–10 pl of 100 µM CAP1-targeting siRNA [5′-CUGUA-UGGAGACGGUUCUU (dTdT)-3′ corresponding to 274–1698 bp of mouse *Cap1* full-length sequence (NM_001301067.2), Bioneer, Daejeon, Korea] was microinjected into the cytoplasm of a fully-grown GV oocyte using an Eppendorf FemtoJet and a Nikon Diaphot ECLIPSE TE300 inverted microscope equipped with a Narishige MM0-202N hydraulic 3-dimensional micromanipulator. After injection, the oocytes were cultured in M16 medium containing 2 µM milrinone for 20 h to ensure knockdown of CAP1, washed five times for 2 min each with fresh M16 medium, transferred to fresh M16 medium, and cultured under paraffin oil at 37°C in an atmosphere of 5% CO_2 in air. Control oocytes were microinjected with 5–10 pl of AccuTarget Control siRNA (SN-1001, Bioneer).

Western blot analysis

A total of 200 mouse oocytes per sample were placed in 1× SDS sample buffer and heated at 99°C for 5 min. Proteins were separated using SDS-PAGE and transferred to polyvinylidene fluoride membranes in 1× transfer buffer. The membranes were blocked in Tris-buffered saline containing 0.1% Tween 20 (TBS-T) and 5% nonfat milk for 1 h, followed by incubation at 48°C overnight with either rabbit anti-CAP1 (1:1000; ab88446, Abcam) or mouse anti-β-tubulin antibodies (1:1000; D3U1W, Cell Signaling Technology). The membranes were washed three times with TBS-T (10 min each) and incubated for 1 h with horseradish peroxidase-conjugated goat anti-rabbit-IgG or anti-mouse-IgG (1:1000; sc-2004 and sc-2005, Santa Cruz Biotechnology). Signals were detected using Pierce ECL western blotting substrate (Thermo Fisher Scientific).

Immunofluorescence analysis

Oocytes were fixed with 3.7% paraformaldehyde (w/v) in phosphate-buffered saline (PBS; P4417, Sigma-Aldrich) containing 0.1% polyvinyl alcohol (PVA), followed by permeabilization with 1% Triton X-100 (v/v) for 20 min at 37°C. After a 1 h incubation in blocking buffer [PBS containing 1% bovine serum albumin (BSA)], the samples were incubated with various antibodies in a blocking buffer overnight at 4°C and washed three times with washing buffer (0.5% Triton X-100 and 0.1% Tween 20 in PBS-PVA). To examine the kinetochore–microtubule attachments, oocytes were briefly chilled at 4°C to induce depolymerization of non-kinetochore microtubules just before fixation. The antibodies used were rabbit anti-CAP1 (1:1000; ab88446, Abcam), rabbit anti-phospho-cofilin (Ser3) (1:1000; 77G2; Cell Signaling Technology) and anti-α-tubulin (1:500; F2168, Sigma-Aldrich). Secondary antibodies were conjugated with Alexa Fluor 488 (1:100; SAB4600234, Sigma-Aldrich) and Alexa Fluor 594 (1:100; SAB4600321, Sigma-Aldrich) for 1–2 h at room temperature and washed three times with washing buffer. To stain the cytoplasmic actin mesh or cortical actin, the oocytes were fixed and stained with phalloidin-tetramethylrhodamine (10 mg/ml; Sigma-Aldrich), which labels F-actin. The oocytes were counterstained with Hoechst 33342 (Sigma Life Science) (10 mg/ml in PBS) for 15 min, mounted on a glass slide, and examined using a Zeiss LSM 710 META confocal laser-scanning microscope.

Construction of recombinant plasmids and *in vitro* transcriptions

For mNeongreen- or mScarlet-fused hCAP1 expression, a construct encoding the human CAP1 open reading frame was obtained from Integrated DNA Technologies (Stokie, Illinois, USA) and cloned into pRN3 vectors (Lemaire et al., 1995), followed by *in vitro* transcription using an mMessage mMachine T3 Kit (Thermo Fisher Scientific, Waltham, MA, USA).

For visualization of the actin filament, GFP–UtrCH was used as an F-actin probe (Burkel et al., 2007), which was obtained from Addgene (26737; Cambridge, MA, USA). pRN3-H2B-mCherry plasmids were kindly provided by Dr JungSoo Oh (Sung Kyun Kwan University, Suwon, Korea).

For the generation of constitutively active cofilin, the serine 3 residue was mutated to an alanine residue to prevent phosphorylation (Moriyama et al., 1996). The corresponding mutated gene was cloned into PCS2+ vectors (Jang et al., 2014), followed by *in vitro* transcription and poly(A) tailing performed with an SP6 mMessage mMachine Kit and a Poly(A) Tailing Kit (Thermo Fisher Scientific).

Time-lapse imaging

Briefly, siRNA, cRNA, cofilin–GFP (S3A), mNeongreen- or mScarlet-fused hCAP1, or GFP–UtrCH mRNAs were microinjected into GV oocytes. After injection, the oocytes were cultured for 20 h in M16 medium containing milrinone to allow for exogenous protein expression. The oocytes were stained with 200 nM of SiR-tubulin (Cytoskeleton, Denver, CO, USA) for 5 h to visualize the spindles. Time-lapse imaging was performed with a confocal laser-scanning microscope (Zeiss LSM 710 META) equipped with a Plan Apochromat 406 1.2 NA water-immersion objective, and a Chamlide observation chamber and incubator system (Live Cell Instrument, Seoul, Korea).

Statistical analyses

Each experiment was performed in triplicate or greater. Statistical analyses were performed with the SPSS software package (version 11.5; SPSS). The significant differences between groups were analyzed using the Student's *t*-test. The data were expressed as the mean±s.e.m., and analysis of variance (ANOVA) was used to analyze the data. *P*-values less than 0.05 were considered statistically significant.

Acknowledgements

The authors thank all group members for their insights and critical reading of the manuscript.

Competing interests

The authors declare no competing or financial interests.

Author contributions

Conceptualization: Z.-L.J., S.N., N.-H.K.; Methodology: S.N.; Formal analysis: Z.-L.J.; Investigation: Z.-L.J., Y.-J.J.; Data curation: Z.-L.J.; Writing - original draft: S.N.; Writing - review & editing: S.N.; Supervision: S.N., N.-H.K.; Funding acquisition: N.-H.K.

Funding

This work was supported by grants from the Rural Development Agency, Republic of Korea, Next Generation Biogreen 21 Program [grant number PJ009594].

Supplementary information

Supplementary information available online at
http://jcs.biologists.org/lookup/doi/10.1242/jcs.222356.supplemental

References

Almonacid, M., Terret, M.-É. and Verlhac, M.-H. (2014). Actin-based spindle positioning: new insights from female gametes. *J. Cell Sci.* **127**, 477-483.

Azoury, J., Lee, K. W., Georget, V., Rassinier, P., Leader, B. and Verlhac, M.-H. (2008). Spindle positioning in mouse oocytes relies on a dynamic meshwork of actin filaments. *Curr. Biol.* **18**, 1514-1519.

Azoury, J., Lee, K. W., Georget, V., Hikal, P. and Verlhac, M.-H. (2011). Symmetry breaking in mouse oocytes requires transient F-actin meshwork destabilization. *Development* **138**, 2903-2908.

Balcer, H. I., Goodman, A. L., Rodal, A. A., Smith, E., Kugler, J., Heuser, J. E. and Goode, B. L. (2003). Coordinated regulation of actin filament turnover by a high-molecular-weight Srv2/CAP complex, cofilin, profilin, and Aip1. *Curr. Biol.* **13**, 2159-2169.

Bernstein, B. W. and Bamburg, J. R. (2010). ADF/cofilin: a functional node in cell biology. *Trends Cell Biol.* **20**, 187-195.

Bertling, E., Hotulainen, P., Mattila, P. K., Matilainen, T., Salminen, M. and Lappalainen, P. (2004). Cyclase-associated protein 1 (CAP1) promotes cofilin-induced actin dynamics in mammalian nonmuscle cells. *Mol. Biol. Cell* **15**, 2324-2334.

Burkel, B. M., von Dassow, G. and Bement, W. M. (2007). Versatile fluorescent probes for actin filaments based on the actin-binding domain of utrophin. *Cell Motil. Cytoskeleton* **64**, 822-832.

Chaigne, A., Campillo, C., Gov, N. S., Voituriez, R., Azoury, J., Umaña-Diaz, C., Almonacid, M., Queguiner, I., Nassoy, P., Sykes, C. et al. (2013). A soft cortex is essential for asymmetric spindle positioning in mouse oocytes. *Nat. Cell Biol.* **15**, 958.

Chaigne, A., Campillo, C., Gov, N. S., Voituriez, R., Sykes, C., Verlhac, M. H. and Terret, M. E. (2015). A narrow window of cortical tension guides asymmetric spindle positioning in the mouse oocyte. *Nat. Commun.* **6**, 6027.

Chaudhry, F., Breitsprecher, D., Little, K., Sharov, G., Sokolova, O. and Goode, B. L. (2013). Srv2/cyclase-associated protein forms hexameric shurikens that directly catalyze actin filament severing by cofilin. *Mol. Biol. Cell* **24**, 31-41.

Deeks, M. J., Rodrigues, C., Dimmock, S., Ketelaar, T., Maciver, S. K., Malhó, R. and Hussey, P. J. (2007). Arabidopsis CAP1 a key regulator of actin organisation and development. *J. Cell Sci.* **120**, 2609-2618.

DesMarais, V., Macaluso, F., Condeelis, J. and Bailly, M. (2004). Synergistic interaction between the Arp2/3 complex and cofilin drives stimulated lamellipod extension. *J. Cell Sci.* **117**, 3499-3510.

Duan, X., Liu, J., Dai, X.-X., Liu, H.-L., Cui, X.-S., Kim, N.-H., Wang, Z.-B., Wang, Q. and Sun, S.-C. (2014). Rho-GTPase effector ROCK phosphorylates cofilin in actin-meditated cytokinesis during mouse oocyte meiosis. *Biol. Reprod.* **90**, 37.

Duan, X., Zhang, Y., Chen, K.-L., Zhang, H.-L., Wu, L.-L., Liu, H.-L., Wang, Z.-B. and Sun, S.-C. (2018). The small GTPase RhoA regulates the LIMK1/2-cofilin pathway to modulate cytoskeletal dynamics in oocyte meiosis. *J. Cell. Physiol.* **233**, 6088-6097.

Dumont, J., Million, K., Sunderland, K., Rassinier, P., Lim, H., Leader, B. and Verlhac, M.-H. (2007). Formin-2 is required for spindle migration and for the late steps of cytokinesis in mouse oocytes. *Dev. Biol.* **301**, 254-265.

Fedor-Chaiken, M., Deschenes, R. J. and Broach, J. R. (1990). SRV2, a gene required for RAS activation of adenylate cyclase in yeast. *Cell* **61**, 329-340.

Field, J., Vojtek, A., Ballester, R., Bolger, G., Colicelli, J., Ferguson, K., Gerst, J., Kataoka, T., Michaeli, T., Powers, S. et al. (1990). Cloning and characterization of CAP, the S. cerevisiae gene encoding the 70 kd adenylyl cyclase-associated protein. *Cell* **61**, 319-327.

Freeman, N. L. and Field, J. (2000). Mammalian homolog of the yeast cyclase associated protein, CAP/Srv2p, regulates actin filament assembly. *Cell Motil. Cytoskeleton* **45**, 106-120.

Holubcová, Z., Howard, G. and Schuh, M. (2013). Vesicles modulate an actin network for asymmetric spindle positioning. *Nat. Cell Biol.* **15**, 937-947.

Hubberstey, A. V. and Mottillo, E. P. (2002). Cyclase-associated proteins: CAPacity for linking signal transduction and actin polymerization. *FASEB J.* **16**, 487-499.

Jang, W.-I., Jo, Y.-J., Kim, H.-C., Jia, J.-L., Namgoong, S. and Kim, N.-H. (2014). Non-muscle tropomyosin (Tpm3) is crucial for asymmetric cell division and maintenance of cortical integrity in mouse oocytes. *Cell Cycle* **13**, 2359-2369.

Jansen, S., Collins, A., Golden, L., Sokolova, O. and Goode, B. L. (2014). Structure and mechanism of mouse cyclase-associated protein (CAP1) in regulating actin dynamics. *J. Biol. Chem.* **289**, 30732-30742.

Jo, Y.-J., Jang, W.-I., Namgoong, S. and Kim, N.-H. (2015). Actin-capping proteins play essential roles in the asymmetric division of maturing mouse oocytes. *J. Cell Sci.* **128**, 160-170.

Jo, Y.-J., Jang, W.-I., Kim, N.-H. and Namgoong, S. (2016). Tropomodulin-3 is essential in asymmetric division during mouse oocyte maturation. *Sci. Rep.* **6**, 29204.

Johnston, A. B., Collins, A. and Goode, B. L. (2015). High-speed depolymerization at actin filament ends jointly catalysed by Twinfilin and Srv2/CAP. *Nat. Cell Biol.* **17**, 1504-1511.

Leader, B., Lim, H., Carabatsos, M. J., Harrington, A., Ecsedy, J., Pellman, D., Maas, R. and Leder, P. (2002). Formin-2, polyploidy, hypofertility and positioning of the meiotic spindle in mouse oocytes. *Nat. Cell Biol.* **4**, 921-928.

Leblanc, J., Zhang, X., McKee, D., Wang, Z.-B., Li, R., Ma, C., Sun, Q.-Y. and Liu, X. J. (2011). The small GTPase Cdc42 promotes membrane protrusion during polar body emission via ARP2-nucleated actin polymerization. *MHR: Basic Sci. Reprod. Med.* **17**, 305-316.

Lemaire, P., Garrett, N. and Gurdon, J. B. (1995). Expression cloning of Siamois, a Xenopus homeobox gene expressed in dorsal-vegetal cells of blastulae and able to induce a complete secondary axis. *Cell* **81**, 85-94.

Mogessie, B. and Schuh, M. (2017). Actin protects mammalian eggs against chromosome segregation errors. *Science* **357**, eaal1647.

Moriyama, K. and Yahara, I. (2002). Human CAP1 is a key factor in the recycling of cofilin and actin for rapid actin turnover. *J. Cell Sci.* **115**, 1591-1601.

Moriyama, K., Iida, K. and Yahara, I. (1996). Phosphorylation of Ser-3 of cofilin regulates its essential function on actin. *Genes Cells* **1**, 73-86.

Namgoong, S. and Kim, N.-H. (2016). Roles of actin binding proteins in mammalian oocyte maturation and beyond. *Cell Cycle* **15**, 1830-1843.

Niwa, R., Nagata-Ohashi, K., Takeichi, M., Mizuno, K. and Uemura, T. (2002). Control of actin reorganization by Slingshot, a family of phosphatases that dephosphorylate ADF/cofilin. *Cell* **108**, 233-246.

Noegel, A. A., Rivero, F., Albrecht, R., Janssen, K. P., Kohler, J., Parent, C. A. and Schleicher, M. (1999). Assessing the role of the ASP56/CAP homologue of Dictyostelium discoideum and the requirements for subcellular localization. *J. Cell Sci.* **112**, 3195-3203.

Ono, S. (2013). The role of cyclase-associated protein in regulating actin filament dynamics - more than a monomer-sequestration factor. *J. Cell Sci.* **126**, 3249-3258.

Pfender, S., Kuznetsov, V., Pleiser, S., Kerkhoff, E. and Schuh, M. (2011). Spire-type actin nucleators cooperate with Formin-2 to drive asymmetric oocyte division. *Curr. Biol.* **21**, 955-960.

Pollard, T. D. and Borisy, G. G. (2003). Cellular motility driven by assembly and disassembly of actin filaments. *Cell* **112**, 453-465.

Pollard, T. D. and Cooper, J. A. (2009). Actin, a central player in cell shape and movement. *Science* **326**, 1208-1212.

Quintero-Monzon, O., Jonasson, E. M., Bertling, E., Talarico, L., Chaudhry, F., Sihvo, M., Lappalainen, P. and Goode, B. L. (2009). Reconstitution and Dissection of the 600-kDa Srv2/CAP Complex. Roles for oligomerization and cofilin-actin binding in driving actin turnover. *J. Biol. Chem.* **284**, 10923-10934.

Sun, Q.-Y. and Schatten, H. (2006). Regulation of dynamic events by microfilaments during oocyte maturation and fertilization. *Reproduction* **131**, 193-205.

Sun, S.-C., Sun, Q.-Y. and Kim, N.-H. (2011a). JMY is required for asymmetric division and cytokinesis in mouse oocytes. *MHR: Basic Sci. Reprod. Med.* **17**, 296-304.

Sun, S.-C., Wang, Z.-B., Xu, Y.-N., Lee, S.-E., Cui, X.-S. and Kim, N.-H. (2011b). Arp2/3 complex regulates asymmetric division and cytokinesis in mouse oocytes. *PLoS ONE* **6**, e18392.

Toshima, J. Y., Horikomi, C., Okada, A., Hatori, M. N., Nagano, M., Masuda, A., Yamamoto, W., Siekhaus, D. E. and Toshima, J. (2016). Srv2/CAP is required for polarized actin cable assembly and patch internalization during clathrin-mediated endocytosis. *J. Cell Sci.* **129**, 367-379.

Wang, Z.-B., Jiang, Z.-Z., Zhang, Q.-H., Hu, M.-W., Huang, L., Ou, X.-H., Guo, L., Ouyang, Y.-C., Hou, Y., Brakebusch, C. et al. (2013). Specific deletion of Cdc42 does not affect meiotic spindle organization/migration and homologous chromosome segregation but disrupts polarity establishment and cytokinesis in mouse oocytes. *Mol. Biol. Cell* **24**, 3832-3841.

Wang, H. Y., Guo, J., Lin, Z. L., Namgoong, S., Oh, J. S. and Kim, N.-H. (2017). Filamin A is required for spindle migration and asymmetric division in mouse oocytes. *FASEB J.* **31**, 3677-3688.

Yi, K. and Li, R. (2012). Actin cytoskeleton in cell polarity and asymmetric division during mouse oocyte maturation. *Cytoskeleton* **69**, 727-737.

Yi, K., Unruh, J. R., Deng, M., Slaughter, B. D., Rubinstein, B. and Li, R. (2011). Dynamic maintenance of asymmetric meiotic spindle position through Arp2/3-complex-driven cytoplasmic streaming in mouse oocytes. *Nat. Cell Biol.* **13**, 1252-1258.

Yi, K., Rubinstein, B., Unruh, J. R., Guo, F., Slaughter, B. D. and Li, R. (2013). Sequential actin-based pushing forces drive meiosis I chromosome migration and symmetry breaking in oocytes. *J. Cell Biol.* **200**, 567-576.

Yu, G., Swiston, J. and Young, D. (1994). Comparison of human CAP and CAP2, homologs of the yeast adenylyl cyclase-associated proteins. *J. Cell Sci.* **107**, 1671-1678.

Yu, J., Wang, C., Palmieri, S. J., Haarer, B. K. and Field, J. (1999). A cytoskeletal localizing domain in the cyclase-associated protein, CAP/Srv2p, regulates access to a distant SH3-binding site. *J. Biol. Chem.* **274**, 19985-19991.

Zhang, H., Ghai, P., Wu, H., Wang, C., Field, J. and Zhou, G.-L. (2013). Mammalian adenylyl cyclase-associated protein 1 (CAP1) regulates cofilin function, the actin cytoskeleton, and cell adhesion. *J. Biol. Chem.* **288**, 20966-20977.

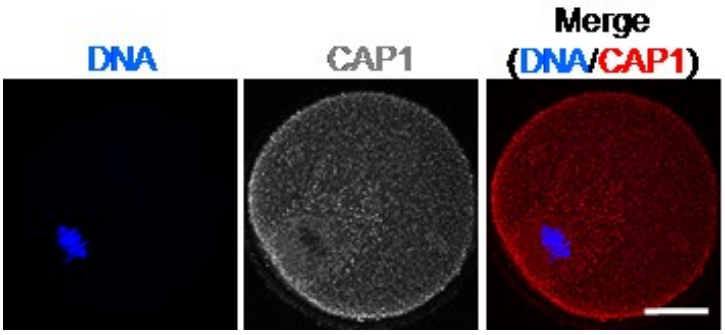

Fig. S1. Subcellular CAP1 localization at MI stage, determined by staining with an anti-CAP1 antibody. CAP1 showed enriched at the cortical actin cap region in MI oocytes. Blue, DNA; red, CAP1. Scale bars: 20 μm (white).

Movie 1. Time-lapse movie of control oocyte injection with H2B-mCherry. Movie 1 correspond to Figure 4A. Maximum intensity z-projection for H2B-mCherry (magenta), with the bright field being shown. The process of movies begins 5 h after the GV stage. The frame interval is 15min. Scale bars: 20 μm

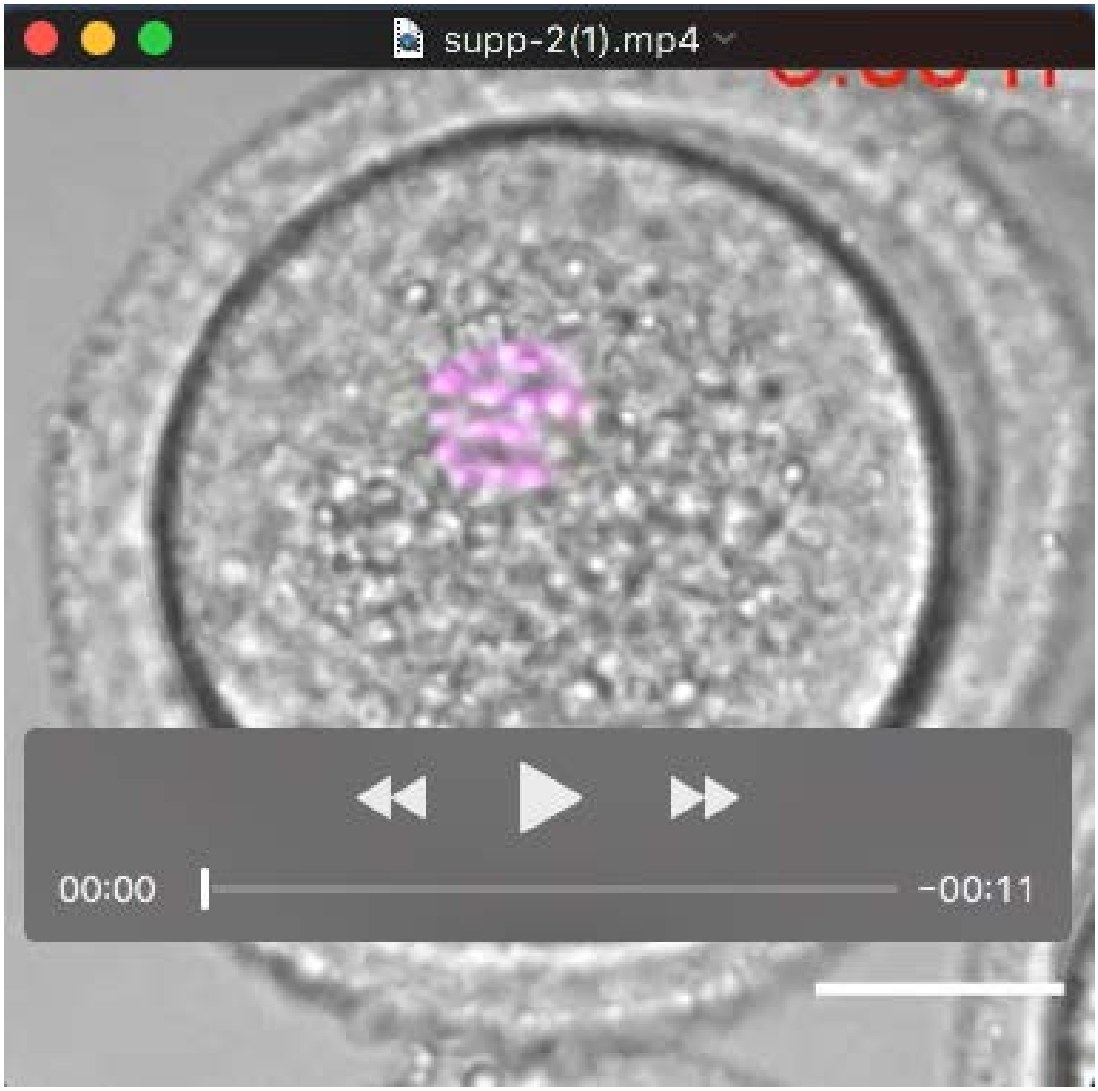

Movie 2. Time-lapse movie of CAP1 KD oocyte injection with H2B-mCherry. Movie 2 correspond to Figure 4A. Maximum intensity z-projection for H2B-mCherry (magenta), with the bright field being shown. The process of movies begins 5 h after the GV stage. The frame interval is 300s. Scale bars: 20 μm

Movie 3. Time-lapse movie of CAP1 KD oocyte injection with H2B-mCherry. Movie 3 correspond to Figure 4A. Maximum intensity z-projection for H2B-mCherry (magenta), with the bright field being shown. The process of movies begins 5 h after the GV stage. The frame interval is 300s. Scale bars: 20 μm

Movie 4. Time-lapse movie of control oocyte injection with H2B-mCherry. Movie 4 correspond to Figure 5H. Maximum intensity z-projection for H2B-mCherry (magenta), with the bright field being shown. The process of movies begins 2 h after the GV stage. The frame interval is 300s. Scale bars: 20 μm

Movie 5. Time-lapse movie of CAP1 overexpression oocyte injection with H2B-mCherry. Movie 5 correspond to Figure 5H. Maximum intensity z-projection for H2B-mCherry (magenta), with the bright field being shown. The process of movies begins 2 h after the GV stage. The frame interval is 300s. Scale bars: 20 μm